JOURNAL OF CIVIL ENGINEERING AND MANAGEMENT
ISSN 1392-3730 / eISSN 1822-3605
2014 Volume 20(4): 466–476
doi:10.3846/13923730.2013.801916

EFFECTS OF VERTICAL SHAFT GEOMETRY ON NATURAL VENTILATION IN URBAN ROAD TUNNEL FIRES

Jie JI, Chuan Gang FAN, Zi He GAO, Jin Hua SUN
State Key Laboratory of Fire Science, University of Science and Technology of China, 230026 Hefei, China
Received 10 Mar 2012; accepted 19 Apr 2012

Abstract. A set of burning experiments were conducted to investigate the effect of vertical shaft geometry on natural ventilation in urban road tunnel fires. Results show that using vertical shafts to discharge smoke leads to a boundary layer separation near the right-angle connection of the shaft and the tunnel ceiling. In a low shaft, the turbulent-boundary-layer separation phenomenon causes relatively large-scale vortexes and restricts smoke from being exhausted, resulting in a negative effect on natural ventilation. Replacing the right-angle connection with the bevel-angle connection was proposed to split one separation point into two separation points, to attenuate the negative effect. The detailed characteristics of the separation phenomenon were analysed and the proposition was verified by Large Eddy Simulation. Results show that there are no relatively large-scale vortexes in shafts with bevel-angle connections, resulting in improved natural ventilation effectiveness. For lower shafts, the advantage of using the bevel-angle connection is more significant, and for shafts of the same height, the mass flow rate of smoke discharged by shafts with the bevel-angle connection increases up to 1.5 times of that by shafts with the right-angle connection. For relatively high shafts, it is about 1.2 times.

Keywords: road tunnel, fire, natural ventilation, vertical shaft, boundary layer separation.

Reference to this paper should be made as follows: Ji, J.; Fan, C. G.; Gao, Z. H.; Sun, J. H. 2014. Effects of vertical shaft geometry on natural ventilation in urban road tunnel fires, *Journal of Civil Engineering and Management* 20(4): 466–476. http://dx.doi.org/10.3846/13923730.2013.801916

Introduction

Nowadays, more and more urban road tunnels are under construction in cities all over the world (Beard 2009). However, owing to the special structure of tunnels, smoke and toxic gases induced by fires such as carbon monoxide, which is the most fatal hazard to people, will not be easily discharged and smoke prohibits safe evacuation of occupants and makes it difficult for firefighters to extinguish the fire. In fact, according to statistics, 85% of deaths in building fires are caused by toxic smoke (Alarie 2002).

In tunnel fires research, the critical velocity and backlayering length due to mechanical ventilation systems (Kunsch 1998; Wu, Bakar 2000; Hwang, Edwards 2005; Roh *et al.* 2007; Van Maele, Merci 2008; Hui *et al.* 2009; Tsai *et al.* 2010), the maximum temperature beneath the ceiling under longitudinal natural wind (Kurioka 2003; Lonnermark, Ingason 2005; Li *et al.* 2011; Ji *et al.* 2012a; Fan *et al.* 2013b) and the heat release rates (Ingason, Lonnermark 2005; Migoya *et al.* 2011) have been widely studied. Relatively few studies have been carried out on smoke movement under the action of natural ventilation with vertical shafts.

When the hot smoke reaches the shaft bottom in the stage of flowing horizontally, the stack effect takes place, and then smoke will be exhausted from the shaft. The more smoke is exhausted by shafts, the lower temperature and smoke spread velocity will be achieved in tunnels, which benefits the evacuation of people. Shafts not only contribute to the discharge of high temperature smoke and weaken its impact on the lining structures and equipments, but also facilitate the airflow exchange between inside and outside of tunnels during daily operation to improve interior air quality.

Several researchers have conducted preliminary studies on the fire-induced smoke flow in road tunnels under natural ventilation with shafts. Wang *et al.* (2009) conducted full-scale experiments on fires in tunnels with roof openings, tested the effect of natural ventilation and investigated the ceiling jet temperature and the backflow distance. Bi *et al.* (2006) studied the effect of natural ventilation with shafts in an urban tunnel employing STAR-CD software and gained the maximum spreading distance of smoke in the tunnel. Yoon *et al.* (2006) investigated the pressure of natural ventilation in the shaft of a road tunnel with results indicating that the natural ventilation pressure induced by the shaft has a significant impact on the efficiency of the ventilation system. However, above studies did not perform detailed analysis on the smoke flow pattern in the shaft and the influence of shaft geometry on the natural ventilation.

The primary driving force of natural ventilation is the stack effect caused by temperature difference of the

Corresponding author: Jie Ji
E-mail: jijie232@ustc.edu.cn

Taylor & Francis
Taylor & Francis Group

shaft compared to the ambient temperature. Its effect mainly depends on the shaft height and the density difference between smoke in the shaft and the ambient air. The pressure difference can be determined by:

$$\Delta P = \Delta \rho g h, \tag{1}$$

where: ΔP is the pressure difference caused by the stack effect (Pa); $\Delta \rho$ is the density difference (kg/m^3); g is the gravity acceleration (m/s^2) and h is the shaft height (m). Smoke of relatively high temperature will induce a strong stack effect, which is in favour of smoke exhausting.

In this paper, a set of burning experiments were conducted originally to investigate the effect of shaft height on natural ventilation in road tunnel fires. It was found that the boundary layer separation could lead to a negative effect on the effectiveness of natural ventilation. Replacing the right-angle connection between the shaft bottom and the tunnel ceiling with the bevel-angle connection was proposed then to split one separation point into two separation points, to attenuate the negative effect on natural smoke exhausting by vertical shafts. Subsequently, the detailed characteristics of the separation phenomenon were analysed and the proposition was verified by Large Eddy Simulation (LES).

1. Experiments

1.1. Experiment setup

The experiments were conducted in a small-scale urban road tunnel model as shown in Figure 1 (Ji *et al.* 2012b; Fan *et al.* 2013a). A scale ratio of 1:6 is applied in current cases. The tunnel is 6 m long, 2 m wide and 0.88 m tall. Its aspect ratio is determined based on a survey of 17 urban road tunnels in Beijing, Nanjing and Shenzhen in China, and is considered to be a general representation.

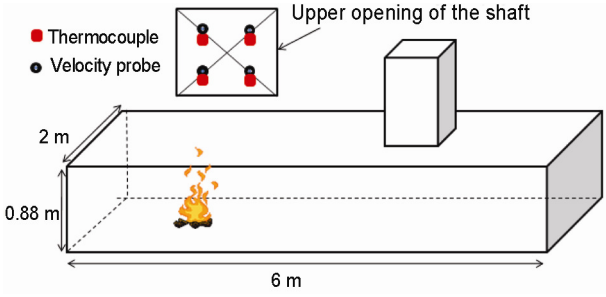

Fig. 1. Schematic of experimental apparatus

The Froude modelling was applied to build up the physical scale model. As the scaling laws of Froude modelling do not apply to conductive and radiative heat transfer processes, it is actually assumed that the heat transfer mechanisms in this research work were predominantly convective (Ji *et al.* 2011). The heat release rate (HRR), Q, the temperature, T and the velocity, V, are scaled using Eqns (2)–(4). L denotes the model size, and the subscript 'm' represents the model tunnel and the subscript 'f' represents the full-scale tunnel.

$$\frac{Q_m}{Q_f} = \left(\frac{L_m}{L_f}\right)^{5/2}; \tag{2}$$

$$T_{\mathrm{m}} = T_f; \tag{3}$$

$$\frac{V_m}{V_f} = \left(\frac{L_m}{L_f}\right)^{1/2}. \tag{4}$$

The distance between the shaft and the left opening of the tunnel is 4.2 m. The cross section of the shaft is 30×30 cm. In the experiments, six shafts were used, with heights of 0 m, 0.2 m, 0.4 m, 0.6 m, 0.8 m and 1.0 m respectively.

Sixteen thermocouples (K-type) with a 1.5 cm vertical interval were positioned vertically under the shaft bottom. Four thermocouples were installed uniformly at the upper opening of the shaft. One velocity probe was set near each thermocouple at the upper opening of the shaft. KANOMAX four channel measurement unit was used for velocity measurements.

Four heat release rates were used in the experiments, which were 20.21 kW, 29.57 kW, 36.66 kW and 44.01 kW. The fire source was located at 1.4 m away from the left end of the model tunnel. The distance from the fire surface to the ceiling was 0.865 m. Methanol was applied as fuel with incense as tracer agent. A laser sheet (with an output power of 2 W and a sheet thickness of 1 mm) was used as a visualization assistant tool to show the flow patterns. A Digital Video was used to record the experimental phenomena.

1.2. Experimental results and discussion

In these cases, the average value of the two velocity probes at the left side of the shaft (near the fire) is considered as the upstream velocity, whereas the average value of the other two velocity probes is regarded as the downstream velocity. The upstream and downstream velocities with different shaft heights are shown in Figure 2.

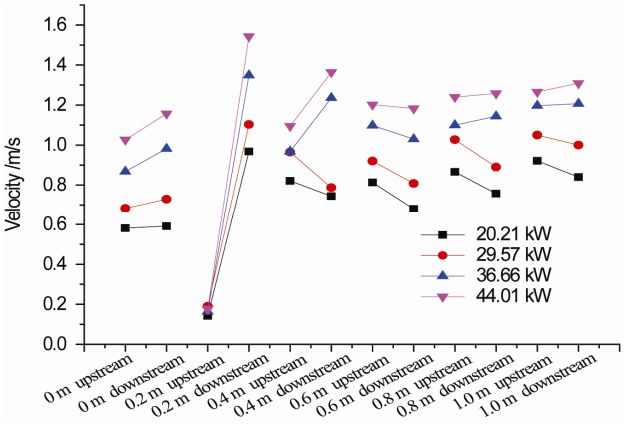

Fig. 2. Upstream and downstream smoke exhausting velocities at the shaft top opening

When the shaft height is 0 m, there is little difference between the upstream and downstream velocities in all experimental cases. When the HRR is relatively low (20.21 kW), the inertia force of smoke layer in the horizontal direction is relatively weak, and the smoke directly flows out from the ceiling opening, resulting in approximately equal upstream and downstream velocities. As the horizontal inertia force increases with the HRR, the difference between the upstream and downstream velocities becomes larger. However, the difference is insignificant.

When the shaft height is 0.2 m, the difference between the upstream and downstream velocities is significantly large. The upstream velocity is approaching to zero, and for the cases with the same HRR, the downstream velocity in 0.2 m high shaft is higher than that of other shaft heights. Figure 3 presents the smoke flow configuration (lightened by the laser sheet) in the vertical shaft in the cases with 29.57 kW and shaft heights of 0.2 m and 0.6 m. As shown in Figure 3a, smoke flows towards the downstream area of the shaft top from the upstream area of the shaft bottom under the combined effect of the horizontal inertia force and buoyancy. There is nearly no smoke at the upstream area of the top opening, resulting in a very small reading of the corresponding velocity probes. As the connection angle of the shaft bottom and the tunnel ceiling is right-angle type, once smoke with horizontal inertia force reaches the shaft bottom and flows into the shaft, it separates from the surface of tunnel and shaft immediately, i.e. the boundary layer separation (Zhuang *et al.* 2009), then smoke flows towards the right wall of the shaft after passing across the separation point.

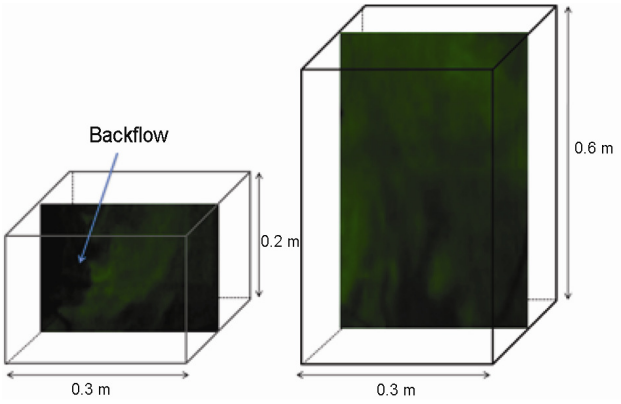

(a) h = 0.2 m (b) h = 0.6 m

Fig. 3. Smoke flow configuration in the vertical center section of the shaft

Once the shaft height is small, the relatively weak stack effect is not able to overcome the adverse pressure gradient, therefore the outside fresh air flows into the shaft, resulting in a backflow in this area. Small amount of smoke flow will be entrained into the backflow and mix with the fresh air. However, large-scale vortexes in the backflow area will entirely constrain the smoke from being exhausted. As a result, smoke can only be discharged from the right part of the shaft, as shown in Figure 3a. The upstream velocity is approaching zero and has a great difference compared to the downstream velocity. The occurrence of the boundary layer separation greatly reduces the effective smoke exhausting area of the vertical shaft and the natural ventilation effectiveness.

When the shaft height is between 0.6 m and 1.0 m, the upstream and downstream velocities at the shaft top opening are more even. The typical smoke flow configuration in the vertical centre section of the shaft is presented in Figure 3b. It is noted that smoke is exhausted from both the upstream and downstream areas of the top opening. As the separation point exists, the boundary layer separation still occurs. However, as the shaft height is relatively high, smoke will keep flowing upwards after being blocked by the vortexes at the right wall of the shaft, and entrain continuously the air near the left wall. When smoke reaches the top opening, the more significant stack effect forms and produces a relatively larger pressure difference, attenuating the negative influence of boundary layer separation on the exhausting process.

In all cases with shaft height of 0.4 m, the upstream velocities are over 0.8 m/s. In cases with a larger HRR (36.66 kW and 44.01 kW), the downstream velocity is nearly 0.4 m/s higher than the upstream velocity. In cases with a lower HRR (20.21 kW and 29.57 kW), the upstream and downstream velocities are generally equivalent. Therefore, it could be concluded that the flow pattern around the shaft height of 0.4 m is in the transition stage between the significantly and slightly negative influences caused by boundary layer separation.

So far, the shape of shafts for natural ventilation in urban road tunnels is commonly cubic, namely the connection angle between the shaft bottom and the tunnel ceiling is 90° as shown in Figure 3 (Wang *et al.* 2009; Yan *et al.* 2009). According to fluid mechanics (Zhuang *et al.* 2009), the angle should be designed as "streamlined" to avoid the occurrence of boundary layer separation. For structures like tunnel shafts, it is unnecessary to design a streamlined connection due to complexity. Huang *et al.* (2011) found that changing the connection angle between the shaft and the tunnel ceiling could enhance the efficiency of air exchange caused by the train piston wind. However, the driving force of airflow in Huang's research is much different from the buoyancy and horizontal inertia force of the smoke ceiling jet. Based on analysis of the boundary layer separation, replacing the right-angle connection between the shaft bottom and the tunnel ceiling with the bevel-angle connection was proposed in this paper, to split one separation point into two separation points, to attenuate the negative effect on natural smoke exhausting caused by the vertical shaft.

2. CFD numerical modelling

2.1. Fire dynamics simulator and fire scenario analysis

The rapid development of computer provides efficient tools for fire safety risk assessment (Chow 1996, 2011; Chow, C., Chow, W. 2009; Chow, Li 2010; Papinigis *et al.* 2010; Tserng *et al.* 2011) such as Computational

Fluid Dynamics (CFD) and in particular LES codes for modelling fires. The software package, Fire Dynamics Simulator (FDS) (Mcgrattan *et al.* 2010), a LES code coupling with a post-processing visualization tool, Smokeview, developed by National Institute of Standards and Technology (NIST), USA, could now be regarded as a practical tool for simulating fire-induced environment. The model has been subjected to numerous validations, calibrations and studies on the temperature and velocity fields in fires (Hwang, Edwards 2005; Roh *et al.* 2007; Kim *et al.* 2008; Hadjisophocleous, Jia 2009; Tilley *et al.* 2011).

Therefore, in the following part, we will not attempt to verify the validity of FDS code by simulating the fire-induced smoke flow in tunnels and comparing our experimental results to simulated results. Instead, the detailed characteristics of the separation phenomenon will be analysed and the proposition of the bevel-angle connection will be tested by the FDS code.

The FDS solves numerically a form of the Navier–Stokes equations for thermally-driven flow. A description of the model, many validation examples, and a bibliography of related papers and reports may be found on http://fire.nist.gov/fds/. It includes both the DNS (Direct Numerical Simulation) model and the LES (Large Eddy Simulation) model. The LES model, which is widely used in study of fire-induced smoke flow behaviour, is selected in this study.

The Sub-Grid-Model (SGM) commonly used in LES is developed originally by Smagorinsky (1963). The eddy viscosity is obtained by assuming that small scales are in equilibrium, by balancing the energy production and dissipation. The Smagorinsky constant C_s in LES simulation is flow dependent and has been optimized over a range from 0.1 to 0.25 for various flow fields. FDS has been subjected to many verification works and improved since its first release in 2000. According to these validation works, the constants, C_s , Pr and Sc, are set as default values in the FDS for current paper as 0.2, 0.2 and 0.5, respectively. It was reported (Jiang, Chen 2003) that for simulating buoyancy-drive flow, the predicted values from the filtered dynamics SGM by FDS agreed better with the measured value than those from the original Smagorinsky model and RANS (Reynolds-Averaged Navier-Stokes) models.

By taking the aspect ratio and shaft size of actual tunnels into account, the model tunnel in current research was specified as 50 m long, 12 m wide and 5.4 m high and the shaft was 3 m long and 3 m wide with a changeable height.

The HRR was specified as 4 MW representing a typical car fire (Ko *et al.* 2010). The fire source was 10 m away from the left end of the tunnel. The shaft was at the right hand side of the fire with a distance of 16 m. In the full-scale experiments conducted by Yan *et al.* (2009), the longitudinal wind velocity was between 0.8 m/s and 1.5 m/s, so in the current model the longitudinal wind velocity was set to be 1.0 m/s. The ambient temperature was 20 °C.

In the FDS simulations, the grid size is a key parameter to be considered. A $D^*/\delta x$ criterion has been widely used for assessing the grid resolution (Mcgrattan *et al.* 2010), where δx is the grid size and the characteristic length of D^* is calculated by:

$$D^* = \left(\frac{\dot{Q}}{\rho_\infty c_p T_\infty \sqrt{g}} \right)^{\frac{2}{5}}. \quad (5)$$

It was recommended by Mcgrattan *et al.* (2010) that the value of $D^*/\delta x$ should be in the range of 4 to 16. Then the grid size of the finest mesh for a 4 MW fire was calculated to be between 0.1 m and 0.4 m. Furthermore, a grid system with smaller grids of 0.13 m assigned near to the fire and larger grids of 0.4 m in other spaces was reported (Mcgrattan, Hamins 2003) to give good predictions on tunnel fire simulations by FDS.

Obviously, finer grid will better reflect the heat flow field in detail, but it is also time consuming. So we have to make a choice for an appropriate mesh grid size. In this paper, six different mesh sizes ranging from 0.1–0.4 m are chosen for comparison. Figure 4 presents the vertical temperature distribution in the tunnel with different grid sizes. With the mesh density increasing, the temperature curve trends to be uniform. The results of mesh with 0.2 m, 0.167 m and 0.1 m have a slight difference, that is to say, there is no significant improvement but it is more time consuming when the mesh size is smaller than 0.2 m. Hence, we choose a multi-mesh system with grid size of 0.1 m in the shaft and fire region and 0.2 m in the other origin.

An inlet velocity boundary condition was set at the left opening of the tunnel domain. The top of the shaft and the right side of the tunnel were set to be naturally opened with no initial velocity boundary condition. In CFD simulation, a model with or without an exterior environment will lead to different simulation results. Therefore, the additional computational regions are added

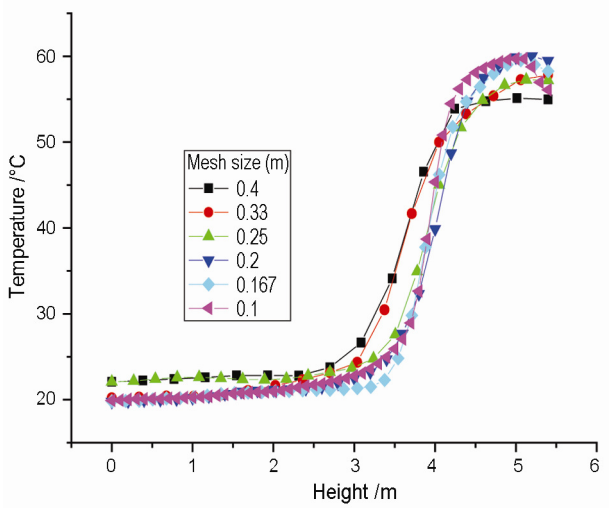

Fig. 4. Vertical temperature distribution in the tunnel with different grid sizes

near the top opening of the vertical shaft and tunnel outlet. The internal lining of the tunnel and shaft was specified as "CONCRETE". The thermal properties of this material are available in the FDS database documentation. The schematic diagram of the model is shown in Figure 5.

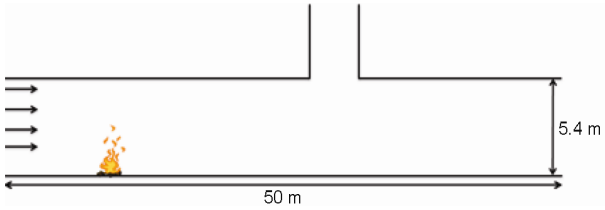

Fig. 5. Model configuration of the tunnel

A data collection point of the mass flow rate was positioned at the top opening of the shaft. The mass flow rate of smoke exhausted from the shaft is regarded as the key factor to judge if the natural ventilation is effective. The shaft heights used in the model were 2.6 m, 4.6 m and 6.6 m. The connection angles between the shaft bottom and the tunnel ceiling (θ) were 90°, 63.4°, 45° and 26.6°, as presented in Figure 6. In the models, it is ensured that all the shafts connected to the tunnel with the bevel-angle have increased the same volume of space to the shaft connected to the tunnel with the right-angle at the same shaft height. As FDS uses structured grids, setting an inclined surface is tedious. Therefore, for the convenience of model setting, two non-integral connection angles, i.e. 63.4° (close to 60°) and 26.6° (close to 30°), were used, and it did not imply that these two non-integral angles were critical values. Actually, Tan(63.4°) = 2 and Tan(26.6°) = 0.5. The computing domain was partly filled by 'CONCRETE' blockages, namely the green zone shown in Figures 9b, c and d to produce the inner cross-sectional dimension of the structure. To reduce the effect of stepping on the flow field near the blockages, the jagged steps were smoothed by the FDS command of ''SAWTOOTH = .FALSE.''. In total, 12 cases were simulated.

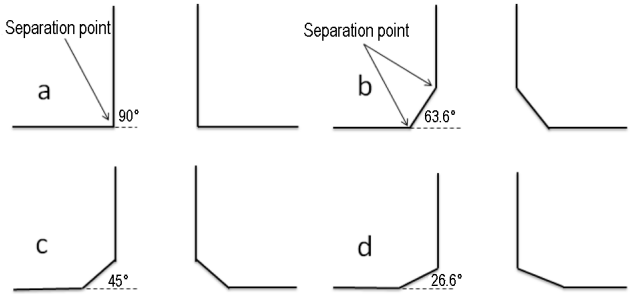

Fig. 6. The connection angle between the shaft and tunnel

2.2. Simulated results and discussion

2.2.1. Right-angle connection

Figure 7 presents the smoke temperature distribution in the shaft and tunnel, where the right side magnifies the isotherm distribution in the shaft (the sidewalls of the shaft are marked with black lines). As shown in Figure 7a, when the shaft height is 2.6 m, the temperature at the right side of the shaft, about 60 °C, is significantly higher than that at the left side, about 25 °C, which is slightly above the ambient temperature.

As shown in Figures 7b and c, with the increase of the shaft height (4.6 m and 6.6 m), the stack effect will become stronger, and more smoke will be discharged. Therefore, the smoke layer thickness under the shaft decreases as the shaft height increases, resulting in one "hollow area" below the shaft. In fact, the "hollow area" is full of fresh air which fills the original smoke region. The shape of the "hollow area" depends on the ratio of the inertia force in vertical direction to the gravity force which is relevant to the buoyant flows associated with fires (Cooper 2002; Jie *et al.* 2010). There is no obvious "hollow area" in Figure 7a, and the top point of the "hollow area" in Figure 7c almost enters the shaft, which indicates that the inertia force in vertical direction generated by the stack effect in case of 6.6 m high shaft is the biggest one in the three cases whereas the case of 2.6 m high shaft gives the smallest inertia force. It also can be seen that the top point of the "hollow area" in Figure 7c is near the right side of the shaft bottom, due to the action of horizontal velocity of the smoke layer. That is different from the case of smoke exhausting in smoke storage space surrounded by solid surface, such as wall, smoke curtain of certain height, etc. In that type of space, there is a smoke layer with certain thickness under ceiling and without evident velocity in horizontal direction, and thus the top point of the "hollow area" under the smoke exhausting vent is located just under the centre of vent (Jie *et al.* 2010). Therefore, the inertia force in horizontal direction also influences the natural smoke exhausting effect and should be also considered, besides the inertia force in vertical direction and the gravity force mentioned above, in design of the natural smoke exhausting system in tunnels. As shown in Figures 7b and c, the disturbance on the smoke-air interface caused by the stack effect, will cause the cold fresh air near smoke-air interface to be mixed with smoke and then exhausted by the vertical shaft. It results in that the temperature over the top point of the "hollow area" is lower than that at the left side of the shaft at the same height. In the upper space inside the shaft, the temperatures at the left and right sides, between 40 and 60 °C, are nearly equal at the same height. It indicates that the smoke and the cold fresh air mix sufficiently in the upper space.

Figure 8 presents the velocity vector field in the shaft when the connection angle is 90°. As shown in Figure 8a, the flow velocity is about zero near the separation point when the shaft height is 2.6 m. Some amount of air outside the shaft flows into it due to the adverse pressure difference, which produces large-scale turbulent vortexes that will block the smoke from being exhausted across the left side of the shaft. The smoke soot field and flow pattern in the shaft are shown in Figure 9a. As only a little amount of smoke flows into the backflow, the smoke concentration at the left side is fairly low. The shaft volume for exhausting actual smoke is only half of the total volume, which leads to a significant reduction of the exhausting effectiveness.

As the shaft height increases, the scale of turbulent vortexes becomes smaller and the vortexes are only presented near the separation point, as shown in Figures 8b and c. In the region above the backflow, the smoke adheres to the left wall surface, namely the boundary layer attachment or the Coanda effect (Zhuang *et al.* 2009). If a smooth fluid flows across a convex surface with certain curvature, it has an adsorption tendency to the convex surface. When the smoke moves upwards in the shaft, it continuously entrains the air whereas the left wall surface of shaft restrains the smoke entrainment, resulting in smoke attachment onto the left side wall. Harrison and Spearpoint (2010) have also observed this phenomenon in the study of adhered spill plume. The stack effect strengthens with the increase of the shaft height, resulting in the smoke exhausting velocity in the shaft increasing and scale of turbulent vortexes decreasing. Therefore, the negative effect of boundary layer separation on smoke exhausting decreases and the improved effectiveness of smoke exhausting is achieved.

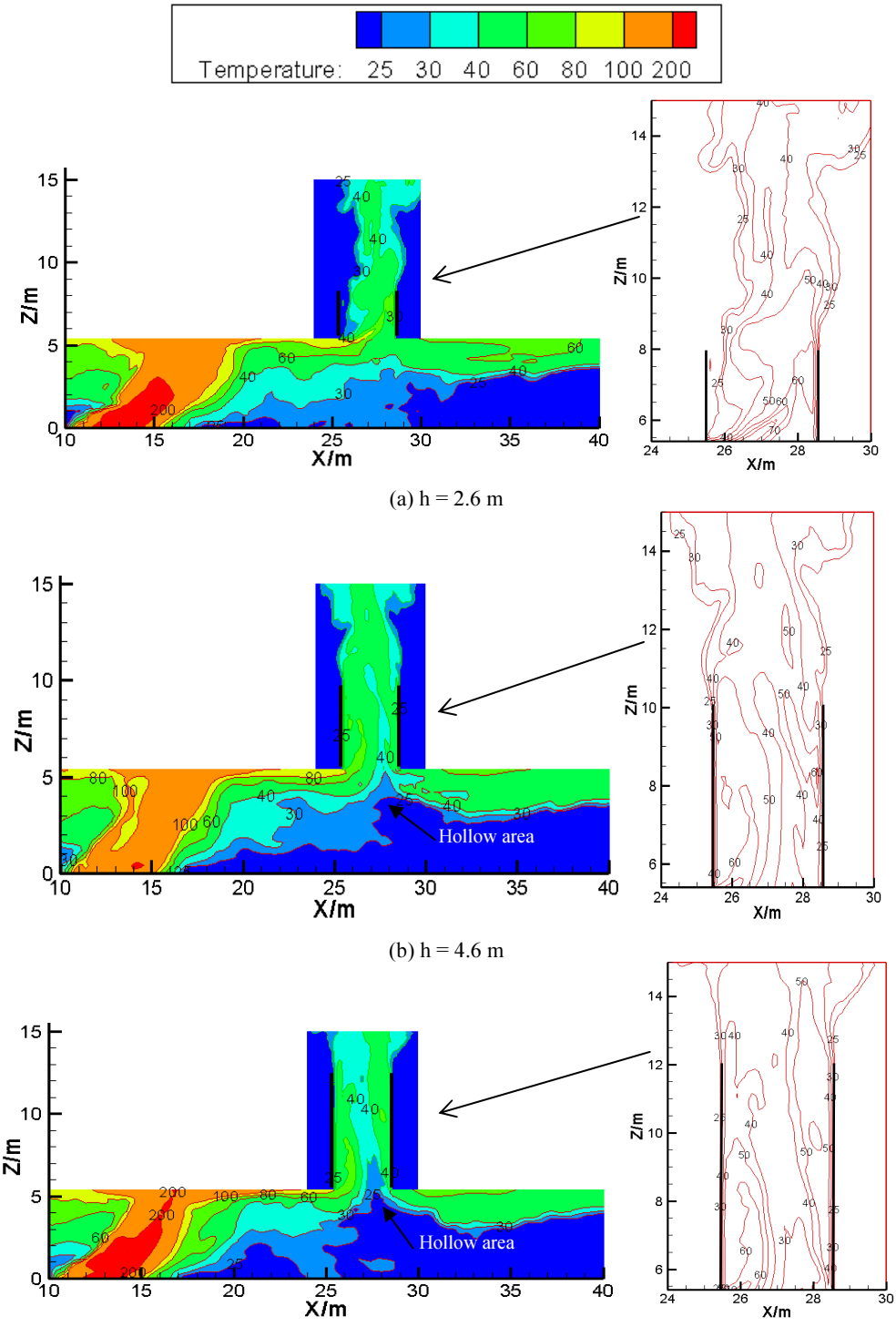

(a) h = 2.6 m

(b) h = 4.6 m

(c) h = 6.6 m

Fig. 7. Temperature field in the shaft and tunnel (the connection angle is 90°)

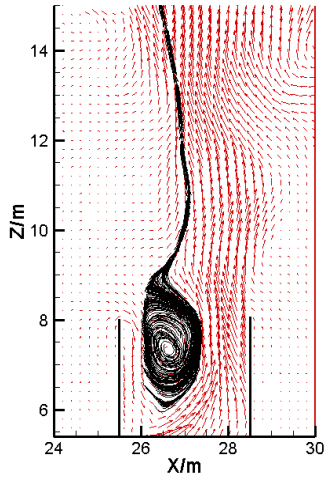

(a) h = 2.6 m

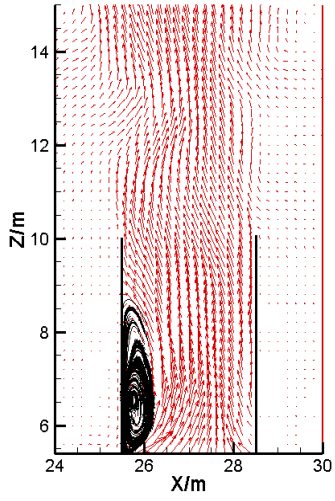

(b) h = 4.6 m

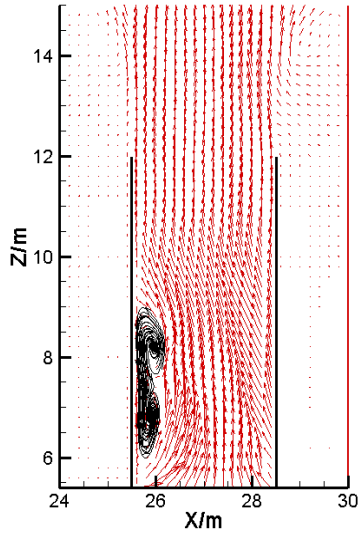

(c) h = 6.6 m

Fig. 8. Velocity vector field in the shaft (the connection angle is 90°)

2.2.2. Bevel-angle connection

Figure 10 presents the smoke temperature profiles in the shaft and tunnel, when the shaft height is 2.6 m. Compared with the Figure 7a (2.6 m high shaft with the right-angle connection), the smoke layer thicknesses under the shaft and at the tunnel downstream decrease, indicating that more smoke is discharged by shaft. The smoke temperature at the left side of the shaft is larger than that at the right side, which is opposite to what Figure 7a shows. The temperature contours at the shaft bottom in Figure 10 are significantly hollow, which are similar to those shown in Figures 7b and c. It indicates the vertical inertia force and velocity of smoke exhausting increase.

The velocity vector fields in shafts connected to the tunnel with the bevel-angle when the shaft height is 2.6 m are shown in Figure 11. Compared to the case, in which the connection angle is 90° shown in Figure 8a, in cases of shafts with the bevel-angle connection there are no large-scale turbulent vortexes that prevent the smoke from being exhausted across the left side of the shaft. Theoretically, just splitting one right-angle separation point into two bevel-angle separation points instead of streamlined design, the boundary layer separation still exists. However, as shown in Figure 11, the region between the two separation points has been completely filled with smoke and the negative effect of boundary layer separation is nearly eliminated. It can also be seen from Figures 9b, c and d that the smoke has fully mixed in the shaft and the smoke concentrations at the left and right sides are almost even, indicating an increase of smoke exhausting effectiveness.

2.2.3. Mass flow rate

The mass flow rates of smoke exhausted by shafts in all cases are shown in Figure 12. At the same connection angle, the mass flow rate increases with the shaft height, because the higher shaft engenders a stronger stack effect and thus exhausts more smoke. At the same shaft height, the mass flow rates of smoke discharged in cases of shafts with the bevel-angle connection are similar and always higher than that of the shafts with the right-angle connection. When the shaft height is 2.6 m, as the obvious boundary layer separation caused by the shaft with the right-angle connection blocks the natural smoke exhausting, the increase of mass flow rate is quite significant after the negative effect of boundary layer separation is basically eliminated by the shaft with bevel-angle connection. The average mass flow rate of smoke discharged by the shaft with the bevel-angle connection is almost 1.5 times that discharged by the shaft with right-angle connection. When the shaft heights are 4.6 m and 6.6 m, the average mass flow rates of smoke discharged by the shafts with the bevel-angle connection are about 1.2 times that discharged by the shafts with the right-angle connection.

It also can be seen from Figure 12 that the mass flow rates of smoke discharged by the 2.6 m high shafts with the bevel-angle connection are slightly higher than that discharged by the 4.6 m high shaft with the right-angle connection. And those discharged by the 4.6 m high shafts

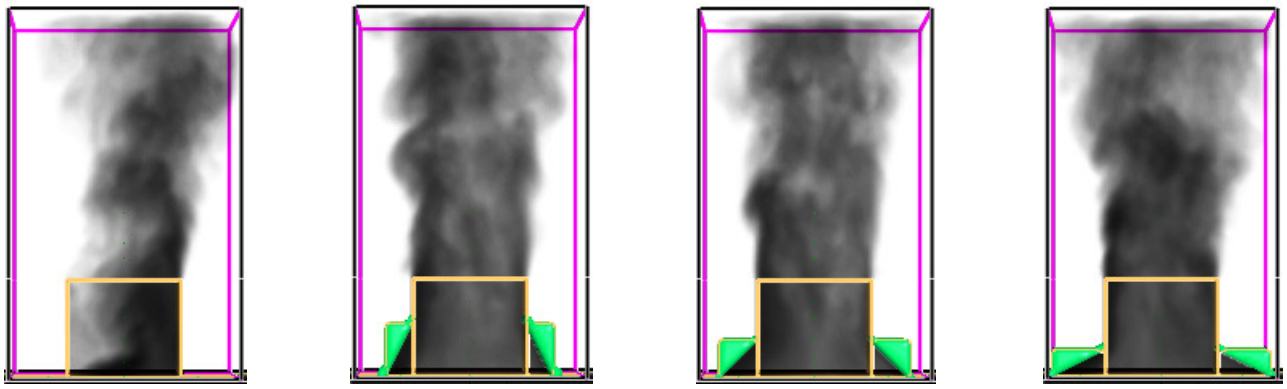

(a) θ = 90° (b) θ = 63.4° (c) θ = 45° (d) θ = 26.6°

Fig. 9. Smoke soot field and flow pattern (the shaft height is 2.6 m)

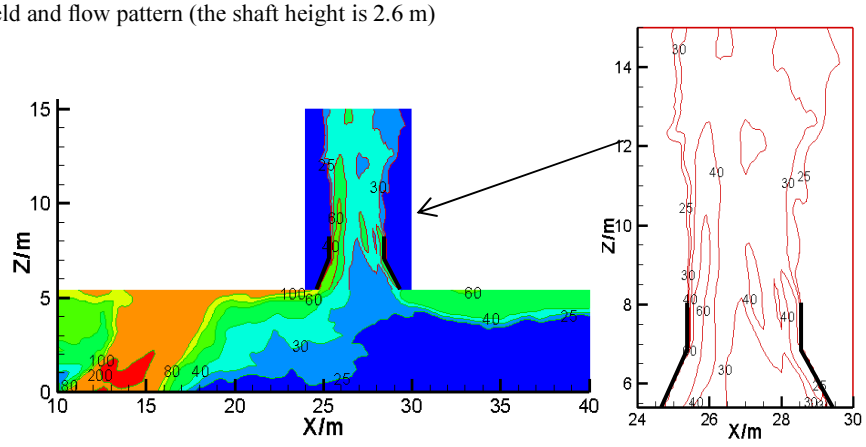

(a) θ = 63.4°

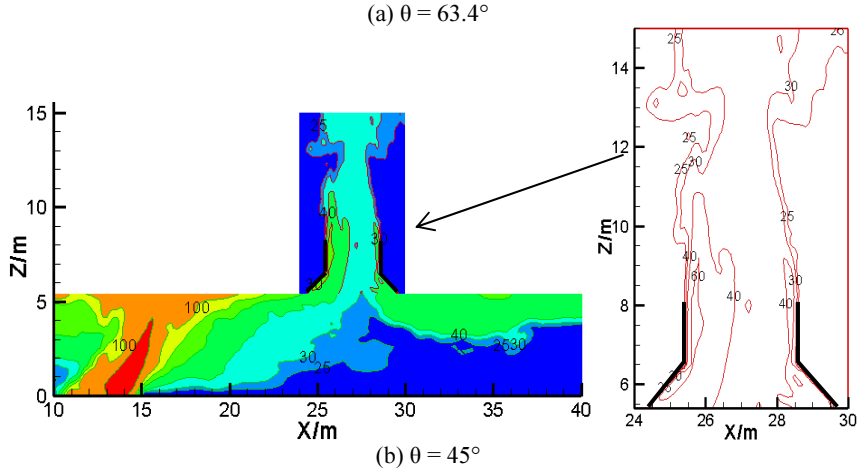

(b) θ = 45°

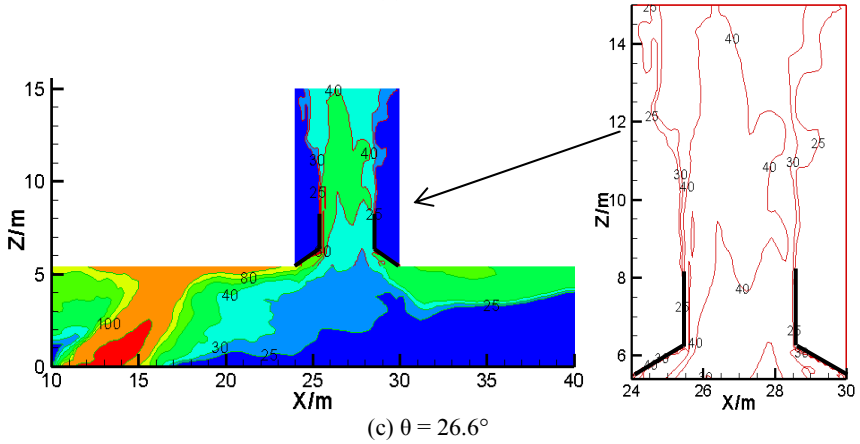

(c) θ = 26.6°

Fig. 10. Temperature field in the shaft and tunnel (the shaft height is 2.6 m)

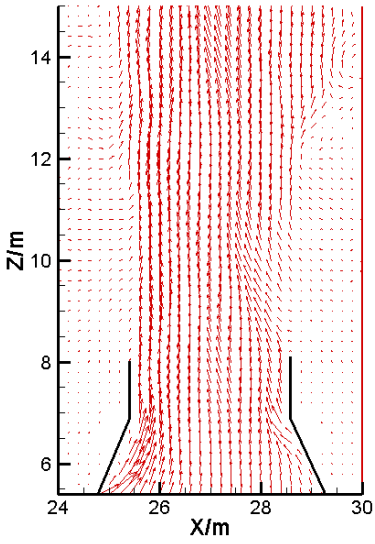

(a) θ = 63.4°

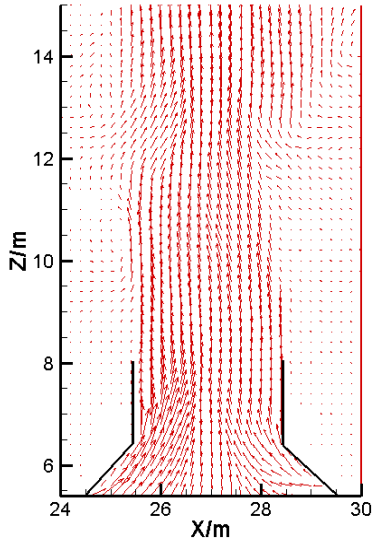

(b) θ = 45°

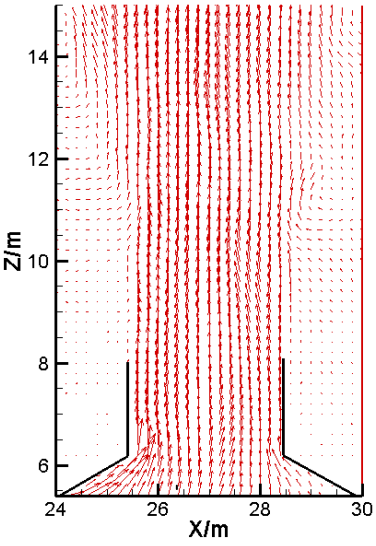

(c) θ = 26.6°

Fig. 11. Velocity vector field in the shaft (the shaft height is 2.6 m)

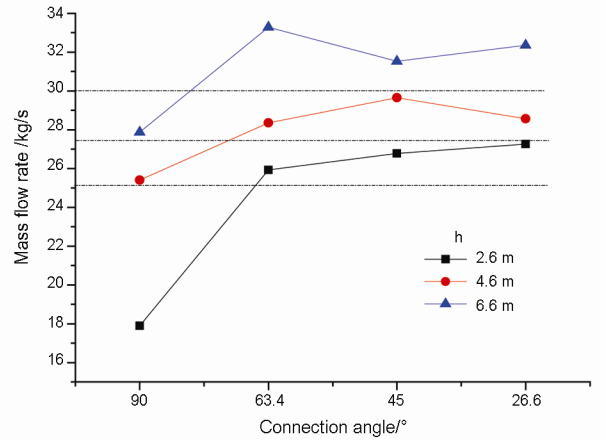

Fig. 12. Mass flow rate of smoke exhausted by the shaft

with the bevel-angle connection are slightly higher than that discharged by the 6.6 m high shaft with the right-angle connection. It can be concluded that once the significant negative effect of the boundary layer separation is eliminated, the natural smoke exhausting effect achieved by a shorter shaft could be better than that achieved by a taller shaft with the right-angle connection. The shaft height and the connection angle should be synthetically considered in practical engineering design, to achieve an optimal natural smoke exhausting effectiveness.

Conclusions

A set of burning experiments were conducted to investigate the effect of vertical shaft geometry on natural ventilation in urban road tunnel fires. Results show that using vertical shafts to discharge smoke leads to a boundary layer separation near the right-angle connection of the shaft and the tunnel ceiling. In the vertical shafts with small height, the turbulent-boundary-layer separation phenomenon causes relatively large-scale vortexes in the vertical shafts and restricts the smoke from being exhausted, resulting in a significant negative effect on natural ventilation. Based on analysis on the boundary layer separation, replacing the right-angle connection between the shaft bottom and the tunnel ceiling with the bevel-angle connection was proposed in this paper, to split one separation point into two separation points, to attenuate the negative effect on natural smoke exhausting by the vertical shaft. Then, the detailed characteristics of the separation phenomenon were analyzed and the proposition was justified by Large Eddy Simulation (LES). Simulated results show that the inertia force in horizontal direction also influences the natural smoke exhausting effect and should be also considered, besides the inertia force in vertical direction and the gravity force, in design of the natural smoke exhausting system in tunnels. There are no relatively large-scale vortexes in vertical shafts with the bevel-angle connection, and the negative impact caused by the boundary layer separation is eliminated in the main, resulting in improved natural ventilation effectiveness. For lower shafts, the advantage of the shafts with the bevel-angle connection is more significant, and for shafts with same heights, the mass flow rate of smoke discharged by the shaft with the bevel-angle con-

nection is increased up to 1.5 times that discharged by shaft with the right-angle connection. For relatively high shafts, it is about 1.2 times. Once the significant negative effect of the boundary layer separation is eliminated, the natural smoke exhausting effect achieved by shorter shaft could be better than that by taller shaft with the right-angle connection. The shaft height and the connection angle should be synthetically considered in practical engineering design, to achieve optimal natural smoke exhausting effectiveness.

Acknowledgement

This work was supported by National Natural Science Foundation of China (NSFC) under Grant No. 51376173 and 50904055, the Anhui Provincial Natural Science Foundation under Grant No. 1208085QE81 and the CAS Special Grant for Postgraduate Research, Innovation and Practice.

Nomenclature

D* – characteristic length (m);
g – gravity acceleration (m/s^2);
h – shaft height (m);
L – model size (m);
ΔP – pressure difference caused by the stack effect (Pa);
Q – heat release rate (kW);
T – smoke temperature (K);
V – smoke velocity (m/s).

Greek symbols

$\Delta\rho$ – density difference (kg/m^3);
θ – connection angle between the shaft and the ceiling (°);
δx – grid size (m).

Subscript

f – full-scale tunnel;
m – model tunnel.

References

Alarie, Y. 2002. Toxicity of fire smoke, *CRC Critical Reviews in Toxicology* 32(4): 259–289.

Beard, A. N. 2009. Fire safety in tunnels, *Fire Safety Journal* 44(2): 276–278. http://dx.doi.org/10.1016/j.firesaf.2008.06.008

Bi, H. Q.; Lei, B.; Zhang, W. H. 2006. Fire smoke flow characteristics in urban road tunnel on natural ventilation mode, in *Proc. of the 2006 International Symposium on Safety Science and Technology. IV, PART A,* 877–881.

Chow, C. L. 2011. Numerical studies on smoke spread in the cavity of a double-skin facade, *Journal of Civil Engineering and Management* 17(3): 371–392. http://dx.doi.org/10.3846/13923730.2011.595075

Chow, C. L.; Chow, W. K. 2009. Fire safety aspects of refuge floors in supertall buildings with computational fluid dynamics, *Journal of Civil Engineering and Management* 15(3): 225–236. http://dx.doi.org/10.3846/1392-3730.2009.15.225-236

Chow, C. L.; Li, J. 2010. An analytical model on static smoke exhaust in Atria, *Journal of Civil Engineering and Management* 16(3): 372–381. http://dx.doi.org/10.3846/jcem.2010.42

Chow, W. 1996. Application of computational fluid dynamics in building services engineering, *Building and Environment* 31(5): 425–436. http://dx.doi.org/10.1016/0360-1323(96)00012-1

Cooper, L. Y. 2002. Smoke and heat venting, in *SFPE Handbook of Fire Protection Engineering.* 3rd ed. Boston, MA, USA, Society of Fire Protection Engineers and National Fire Protection Association.

Fan, C. G.; Ji, J.; Gao, Z. H.; Han, J. Y.; Sun, J. H. 2013a. Experimental study of air entrainment mode with natural ventilation using shafts in road tunnel fires, *International Journal of Heat and Mass Transfer* 56(1–2): 750–757. http://dx.doi.org/10.1016/j.ijheatmasstransfer.2012.09.047

Fan, C. G.; Ji, J.; Gao, Z. H.; Sun, J. H. 2013b. Experimental study on transverse smoke temperature distribution in road tunnel fires, *Tunnelling and Underground Space Technology* 37: 89–95. http://dx.doi.org/10.1016/j.tust.2013.04.005

Hadjisophocleous, G.; Jia, Q. 2009. Comparison of FDS prediction of smoke movement in a 10-storey building with experimental data, *Fire Technology* 45(2): 163–177. http://dx.doi.org/10.1007/s10694-008-0075-3

Harrison, R.; Spearpoint, M. 2010. Physical scale modelling of adhered spill plume entrainment, *Fire Safety Journal* 45(3): 149–158. http://dx.doi.org/10.1016/j.firesaf.2010.02.005

Huang, Y.-d.; Gong, X.-l.; Peng, Y.-j.; Lin, X.-y.; Kim, C.-N. 2011. Effects of the ventilation duct arrangement and duct geometry on ventilation performance in a subway tunnel, *Tunnelling and Underground Space Technology* 26(6): 725–733. http://dx.doi.org/10.1016/j.tust.2011.05.005

Hui, Y.; Li, J.; Lixin, Y. 2009. Numerical analysis of tunnel thermal plume control using longitudinal ventilation, *Fire Safety Journal* 44(8): 1067–1077. http://dx.doi.org/10.1016/j.firesaf.2009.07.006

Hwang, C. C.; Edwards, J. C. 2005. The critical ventilation velocity in tunnel fires – a computer simulation, *Fire Safety Journal* 40(3): 213–244. http://dx.doi.org/10.1016/j.firesaf.2004.11.001

Ingason, H.; Lonnermark, A. 2005. Heat release rates from heavy goods vehicle trailer fires in tunnels, *Fire Safety Journal* 40(7): 646–668. http://dx.doi.org/10.1016/j.firesaf.2005.06.002

Yan, T.; MingHeng, S.; YanFeng, G.; JiaPeng, H. 2009. Full-scale experimental study on smoke flow in natural ventilation road tunnel fires with shafts, *Tunnelling and Underground Space Technology* 24(6): 627–633. http://dx.doi.org/10.1016/j.tust.2009.06.001

Yoon, C. H.; Kim, M. S.; Kim, J. 2006. The evaluation of natural ventilation pressure in Korean long road tunnels with vertical shafts, *Tunnelling and Underground Space Technology* 21(3–4): 472. http://dx.doi.org/10.1016/j.tust.2005.12.108

Ji, J.; Zhong, W.; Li, K. Y.; Shen, X. B.; Zhang, Y.; Huo, R. 2011. A simplified calculation method on maximum smoke temperature under the ceiling in subway station fires, *Tunnelling and Underground Space Technology* 26(3): 490–496. http://dx.doi.org/10.1016/j.tust.2011.02.001

Ji, J.; Fan, C. G.; Zhong, W.; Shen, X. B.; Sun, J. H. 2012a. Experimental investigation on influence of different transverse fire locations on maximum smoke temperature under the tunnel ceiling, *International Journal of Heat and Mass Transfer* 55(17–18): 4817–4826. http://dx.doi.org/10.1016/j.ijheatmasstransfer.2012.04.052

Ji, J.; Gao, Z. H.; Fan, C. G.; Zhong, W.; Sun, J. H. 2012b. A study of the effect of plug-holing and boundary layer separation on natural ventilation with vertical shaft in urban road tunnel fires, *International Journal of Heat and Mass Transfer* 55(21–22): 6032–6041. http://dx.doi.org/10.1016/j.ijheatmasstransfer.2012.06.014

Jiang, Y.; Chen, Q. 2003. Buoyancy-driven single-sided natural ventilation in buildings with large openings, *International Journal of Heat and Mass Transfer* 46(6): 973–988. http://dx.doi.org/10.1016/S0017-9310(02)00373-3

Jie, J.; Kaiyuan, L.; Wei, Z.; Ran, H. 2010. Experimental investigation on influence of smoke venting velocity and vent height on mechanical smoke exhaust efficiency, *Journal of Hazardous Materials* 177(1–3): 209–215. http://dx.doi.org/10.1016/j.jhazmat.2009.12.019

Kim, E.; Woycheese, J. P.; Dembsey, N. A. 2008. Fire dynamics simulator (version 4.0) simulation for tunnel fire scenarios with forced, transient, longitudinal ventilation flows, *Fire Technology* 44(2): 137–166. http://dx.doi.org/10.1007/s10694-007-0028-2

Ko, J.-s.; Yoon, C.-h.; Yoon, S.-w.; Kim, J. 2010. Determination of the applicable exhaust airflow rate through a ventilation shaft in the case of road tunnel fires, *Safety Science* 48(6): 722–728. http://dx.doi.org/10.1016/j.ssci.2010.02.007

Kunsch, J. 1998. Critical velocity and range of a fire-gas plume in a ventilated tunnel, *Atmospheric Environment* 33(1): 13–24. http://dx.doi.org/10.1016/S1352-2310(98)00118-6

Kurioka, H. 2003. Fire properties in near field of square fire source with longitudinal ventilation in tunnels, *Fire Safety Journal* 38(4): 319–340. http://dx.doi.org/10.1016/S0379-7112(02)00089-9

Li, J. 2003. Numerical studies on performance evaluation of tunnel ventilation safety systems, *Tunnelling and Underground Space Technology* 18(5): 435–452. http://dx.doi.org/10.1016/S0886-7798(03)00023-3

Li, Y. Z.; Lei, B.; Ingason, H. 2011. The maximum temperature of buoyancy-driven smoke flow beneath the ceiling in tunnel fires, *Fire Safety Journal* 46(4): 204–210. http://dx.doi.org/10.1016/j.firesaf.2011.02.002

Lonnermark, A.; Ingason, H. 2005. Gas temperatures in heavy goods vehicle fires in tunnels, *Fire Safety Journal* 40(6): 506–527. http://dx.doi.org/10.1016/j.firesaf.2005.05.003

Mcgrattan, K. B.; Hamins, A. 2003. *Numerical Simulation of the Howard Street Tunnel Fire, Baltimore, Maryland, July 2001*. Spent Fuel Project Office, Office of Nuclear Material Safety and Safeguards, US Nuclear Regulatory Commission.

Mcgrattan, K. B.; McDermott, R.; Hostikka, S.; Floyd, J. E. 2010. *Fire dynamics simulator (version5) user's guide*. Gaithersburg, Maryland, National Institute of Standards and Technology.

Migoya, E.; Garcia, J.; Crespo, A.; Gago, C.; Rubio, A. 2011. Determination of the heat release rate inside operational road tunnels by comparison with CFD calculations, *Tunnelling and Underground Space Technology* 26(1): 211–222. http://dx.doi.org/10.1016/j.tust.2010.05.001

Papinigis, V.; Geda, E.; Lukošius, K. 2010. Design of people evacuation from rooms and buildings, *Journal of Civil Engineering and Management* 16(1): 131–139. http://dx.doi.org/10.3846/jcem.2010.12

Roh, J. S.; Ryou, H. S.; Kim, D. H.; Jung, W. S.; Jang, Y. J. 2007. Critical velocity and burning rate in pool fire during longitudinal ventilation, *Tunnelling and Underground Space Technology* 22(3): 262–271. http://dx.doi.org/10.1016/j.tust.2006.08.003

Smagorinsky, J. 1963. General circulation experiments with the primitive equations, *Monthly Weather Review* 91(3): 99–164. http://dx.doi.org/10.1175/1520-0493(1963)091

Tilley, N.; Rauwoens, P.; Merci, B. 2011. Verification of the accuracy of CFD simulations in small-scale tunnel and atrium fire configurations, *Fire Safety Journal* 46(4): 186–193. http://dx.doi.org/10.1016/j.firesaf.2011.01.007

Tsai, K. C.; Chen, H. H.; Lee, S. K. 2010. Critical ventilation velocity for multi-source tunnel fires, *Journal of Wind Engineering and Industrial Aerodynamics* 98(10–11): 650–660. http://dx.doi.org/10.1016/j.jweia.2010.06.006

Tserng, H. P.; You, J. Y.; Chang, C. Y.; Hsiung, K. H. 2011. The hot area evacuation model application in large scale gymnasiums, *Journal of Civil Engineering and Management* 17(2): 217–226. http://dx.doi.org/10.3846/13923730.2011.574461

Van Maele, K.; Merci, B. 2008. Application of RANS and LES field simulations to predict the critical ventilation velocity in longitudinally ventilated horizontal tunnels, *Fire Safety Journal* 43(8): 598–609. http://dx.doi.org/10.1016/j.firesaf.2008.02.002

Wang, Y.; Jiang, J.; Zhu, D. 2009. Full-scale experiment research and theoretical study for fires in tunnels with roof openings, *Fire Safety Journal* 44(3): 339–348. http://dx.doi.org/10.1016/j.firesaf.2008.08.001

Wu, Y.; Bakar, M. 2000. Control of smoke flow in tunnel fires using longitudinal ventilation systems-a study of the critical velocity, *Fire Safety Journal* 35(4): 363–390. http://dx.doi.org/10.1016/S0379-7112(00)00031-X

Zhuang, L. C.; Yin, X. Y.; Ma, H. Y. 2009. *Fluid Mechanics*. Hefei, Anhui, China, University of Science and Technology of China Press.

Jie JI completed his PhD degree in Fire Safety Engineering from SKLFS (State Key Laboratory of Fire Science) at University of Science and Technology of China in 2008. He is an Associate Professor at SKLFS, whose research interests include smoke movement and ventilation control method in building fires and characteristics of flame spread over surface of solid combustibles.

Chuan Gang FAN is a Doctoral Student specializing in Fire Safety Engineering at University of Science and Technology of China from September 2010 to present. His research interests include smoke spread and control for underground buildings and computational fluid dynamics.

Zi He GAO is a Doctoral Student specializing in Fire Safety Engineering at State Key Laboratory of the Fire Science, University of Science and Technology of China. His research interests include fire dynamics, computational fluid and combustion dynamics.

Jin Hua SUN is a Professor at SKLFS (State Key Laboratory of Fire Science), University of Science and Technology of China, and Director of the International Association for Fire Safety Science from 2008 to present. To date, he has authored over 200 research papers, of which 100 were indexed by SCI and EI, including over 20 published in h-factor top journals and six books. His main research interests are fire dynamics and basic fire prevention technologies, large-scale evacuation and rescue in emergencies, hazardous chemical disaster prediction and prevention methods